Superconducting Qubits as Mechanical Quantum Engines

Kewin Sachtleben, Kahio T. Mazon, and Luis G. C. Rego
Department of Physics, Universidade Federal de Santa Catarina, 88040-900 Florianópolis, Santa Catarina, Brazil
(Received 9 February 2017; published 31 August 2017)

We propose the equivalence of superconducting qubits with a pistonlike mechanical quantum engine. The work reports a study on the nature of the nonequilibrium work exchanged with the quantum-nonadiabatic working medium, which is modeled as a multilevel coupled quantum well system subject to an external control parameter. The quantum dynamics is solved for arbitrary control protocols. It is shown that the work output has two components: one that depends instantaneously on the level populations and another that is due to the quantum coherences built in the system. The nonadiabatic coherent dynamics of the quantum engine gives rise to a resistance (friction) force that decreases the work output. We consider the functional equivalence of such a device and a rf-SQUID flux qubit.

DOI: 10.1103/PhysRevLett.119.090601

Technology has evolved to the point where it is possible to design and build mesoscopic machines and molecular motors. Nature has already accomplished that, countless molecular structures operate as engines to sustain life. The most well known are the photosynthetic units [1], the light sensors in the rhodopsin membrane [2], and various molecular proton pumps. Moreover, experiments indicate that nature may use coherences to improve the efficiency of such processes—for instance, quantum coherences for light harvesting in photosynthesis [1,3] and vibrational coherences for phototransduction in visual reception [2,4]. There is, likewise, a great interest to incorporate quantum coherent dynamics into man-made nanomachines and quantum engines—including quantum computers and alike—for both fundamental research and technological applications. Presently, superconducting (SC) circuits based on Josephson junctions are amongst the most promising to produce quantum engines of mesoscopic size [5–8]. For the operation of quantum engines, the most sensitive issues are the coupling with the external control, the nonadiabatic effects caused by the finite time operation [9–11], decoherence caused by interaction with the environment, and energy fluctuations due to the smallness of the device and the nonequilibrium operation regime [12,13]. Fluctuation theorems based on time reversal symmetry provide the theoretical basis to describe the thermodynamics of small systems of both classical [14] and quantum [15,16] nature, for they reconcile the apparent irreversible arrow of time with the underlying reversible microscopic laws.

The main application in the prospect for SC circuits is quantum computation; therefore, such devices are generally treated as qubits, or simply as artificial atoms. However, in view of Landauer's principle for energy consumption of computation, SC-based logical circuits should also be considered quantum engines, subject to energy and entropy exchange. We investigate the properties of a pistonlike quantum engine and explore its correspondence to Josephson qubit circuits. The system consists of a quantum working medium—for instance, an ideal quantum gas—confined by a deformable double-quantum-well (DQW) system that allows for tunneling. The quantum system is driven by an external control parameter and undergoes a finite time unitary process. Its full quantum-nonadiabatic dynamics is solved for an arbitrary control protocol and energy level structure. We examine the difference between thermodynamic and microscopy reversibility, the quantum content of a work stroke, and the origin of the inner friction in quantum thermodynamic processes. The energy fluctuations of the system during cyclic work strokes are analyzed in terms of the quantum Bochkov-Kuzovlev-Jarzynski work fluctuation formalism [14,17,18].

Model system.—Let us consider a quantum particle of mass m dwelling in a DQW system where tunneling is allowed between the wells. We assume that work can be performed on the quantum system by changing the width of one of the wells, like in a piston; different work protocols can be considered for that matter as well. The Hamiltonian of the system is therefore

$$\mathcal{H}(\hat{x};\lambda(t)) = -\frac{\hbar^2}{2m}\frac{d^2}{dx^2} + V_L(\hat{x}) + V_R(\hat{x};\lambda(t)), \quad (1)$$

where $V_L(\hat{x})$ is the potential of the static quantum well, on the left (L). The right-side (R) quantum well is coupled to the work repository through the parameter $\lambda(t) \equiv \mathrm{d}_R(t)$ that represents its width. The deformable potential is written in terms of Heaviside functions $\Theta(x)$ as

$$V_R(\hat{x};\lambda(t)) = V[\Theta(\hat{x}-\lambda(t)) - \Theta(\hat{x})]. \quad (2)$$

The complete adiabatic basis is comprised of all the instantaneous eigenstates of the Hamiltonian, $\mathcal{H}(\lambda_t)|\phi_n(\lambda_t)\rangle = \mathcal{E}_n(\lambda_t)|\phi_n(\lambda_t)\rangle$, where $\lambda(t) \equiv \lambda_t$, including the states of the continuum. In the following we will

consider a unitary transformation, driven by the external parameter $\lambda(t)$, that changes the Hamiltonian from an initial configuration $\mathcal{H}_i = \mathcal{H}[\lambda_i]$ to a final $\mathcal{H}_f = \mathcal{H}[\lambda_f]$ in a finite time interval τ. The process is defined by the time variation of the parameter $\lambda(t)$ and it is described in Fig. 1. The mechanism is analogous to the behavior of rf-SQUID flux qubits [19,20], although the only necessary ingredient is the Landau-Zener transitions.

During a work stroke driven by $\lambda(t)$, the unitary evolution of a given quantum state $|\Psi(t)\rangle = \sum_n C_n(t)|\phi_n(\lambda_t)\rangle$, written in the representation of the adiabatic eigenstates, is given by the time-dependent Schrödinger equation (TDSE), which assumes the form

$$\frac{dC_n}{dt} + \sum_m C_m \langle \phi_n | \dot{\phi}_m \rangle = -\frac{i}{\hbar}\mathcal{E}_n C_n. \tag{3}$$

The nonadiabatic coupling term $\langle \phi_n | \dot{\phi}_m \rangle$ in Eq. (3) describes the transitions amongst the adiabatic eigenstates due to the finite time process. We solve Eq. (3) by means of a general method, also applied for nonadiabatic simulations of excited state quantum dynamics of molecular systems [21,22]. Herein time is discretized in small slices δt, so that $t_j = j\delta t$, with $\delta t \to 0$, which is ensured by verifying that simulations have converged. The instantaneous eigenvalue equation is $\mathcal{H}^{(j)}|\phi_n^{(j)}\rangle = \mathcal{E}_n^{(j)}|\phi_n^{(j)}\rangle$. Thus for a vanishing time slice δt the corresponding Hamiltonian $\mathcal{H}^{(j)} \equiv \mathcal{H}(j\delta t)$ can be assumed constant. Therefore, within that time slice, the adiabatic time-evolution operator assumes the simple form

$$\mathcal{U}_{\mathrm{AD}}|\Psi(t_j)\rangle = \sum_n C_n(t_j)\exp[-i\mathcal{E}_n^{(j)}\delta t/\hbar]|\phi_n^{(j)}\rangle. \tag{4}$$

Operator $\mathcal{U}_{\mathrm{AD}}$ does not describe nonadiabatic effects. To take that into account we make use of the nonadiabatic coupling term

$$\mathcal{U}_{\mathrm{NA}} = \sum_{n,m}\Omega_{n,m}|\phi_m^{(j+1)}\rangle\langle\phi_n^{(j)}|, \tag{5}$$

where

$$\Omega_{n,m} = \langle\phi_m^{(j+1)}|\phi_n^{(j)}\rangle \approx \delta_{n,m} + \langle\dot{\phi}_m^{(j)}|\phi_n^{(j)}\rangle\delta t. \tag{6}$$

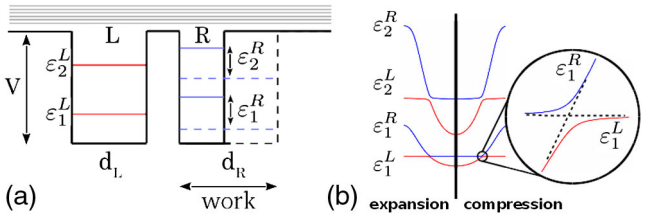

FIG. 1. (a) Energy level scheme of a double quantum well (DQW) system. The left well (L) remains static while the right one (R) exchanges energy with a work repository. There is a quasicontinuum of energy states above the wells. (b) Dynamics of the adiabatic energy levels for the DQW system, $\mathcal{E}_n(\lambda_t)$. For $d_L = d_R$, Landau-Zener (LZ) gaps arise, as shown in the inset.

The term $\Omega_{n,m}$ can be calculated directly from Eq. (6), by using the adiabatic eigenstates at successive time slices. Therefore, the overall time evolution operator $\mathcal{U} = \mathcal{T}\exp[-i\int_0^\tau \mathcal{H}[\lambda(t)]dt/\hbar]$, where $\mathcal{T}$ stands for the time-ordering operator, becomes

$$|\Psi(t_{j+1})\rangle = [\mathcal{U}(t_{j+1},t_j)\ldots\mathcal{U}(t_2,t_1)\mathcal{U}(t_1,t_0)]|\Psi(t_0)\rangle, \tag{7}$$

with $\mathcal{U}(t_{j+1},t_j) = \mathcal{U}_{\mathrm{NA}}(t_{j+1},t_j)\mathcal{U}_{\mathrm{AD}}(t_j)$. To analyze the reversibility properties of the system, we consider a work stroke consisting of an integer number of expansion-and-compression cycles, with the cycles performed at the frequency $\omega_n^{\mathrm{res}} \equiv \min\{|\mathcal{E}_n^R - \mathcal{E}_n^L|\}/\hbar$. For our system, it has been observed that this frequency maximizes the quantum coherence effects during the Landau-Zener (LZ) passage; there are, nonetheless, various definitions of transition times in the LZ model [23]. For a nonautonomous quantum system [16], such as the one discussed here, the microreversibility can be observed by performing the forward work stroke (expansion) from $t = 0$ to $t_f = \tau/2$ with the unitary operator $\mathcal{U}(\tau/2,0)$, then reverting all the momenta with the time-reversal operator ($\mathcal{R}$) as $\Psi(\tau/2) \to \mathcal{R}\Psi(\tau/2) = \Psi^*(\tau/2)$ and, finally, performing the reverse work stroke (compression) given by $\mathcal{U}(\tau,\tau/2) = \mathcal{R}^\dagger\mathcal{U}(\tau/2,0)\mathcal{R}$. That is simply the expansion-and-compression cycle that comprises a complete work stroke. The control protocol for nonautonomous reversibility must obey the condition $\lambda_R(t) = \lambda_F(\tau/2 - t)$, where R and F stand for reverse and forward processes. An analogous approach to test time reversal symmetry has been discussed in detail for charge qubit systems [24].

Figures 2(a) and 2(b) show the microreversibility effect for a particle starting at the first ($n = 1$) and second ($n = 2$) levels of the left QW, respectively. We plotted the particle occupation on the left, $P_n^L = \int_{-\infty}^0 |\Psi(x)|^2 dx$, and on the right, $P_n^R = \int_0^\infty |\Psi(x)|^2 dx$, which is equivalent to the diabatic state representation. Stueckelberg oscillations are clearly observed in the P_n^L and P_n^R curves after each LZ passage, which have also been observed in mesoscopic flux [25,26] and charge [27] SC qubits for analogous control protocols. The dashed line shows the microreversibility effect whereas the continuous line shows evolution without time reversal during the same cycle. For a quantum adiabatic process ($\omega \ll \omega^{\mathrm{res}}$) both dynamics coincide. The autocorrelation function $\mathcal{A}(t) = \langle\Psi(0)|\Psi(t)\rangle$ (see Supplemental Material [28]) corroborates the effect. The irreversible character of the process is caused by the nonadiabatic transitions that accumulate during LZ passages, so that after a complete expansion-compression cycle the system moves away from the initial state.

Work exchange.—Assume that the quantum system has been thermalized with a thermal reservoir at temperature T. The first measurement of $\mathcal{H}(\lambda_0)$ is performed, with results $\mathcal{E}_k(\lambda_0)$. Therefore the system is described by the density matrix

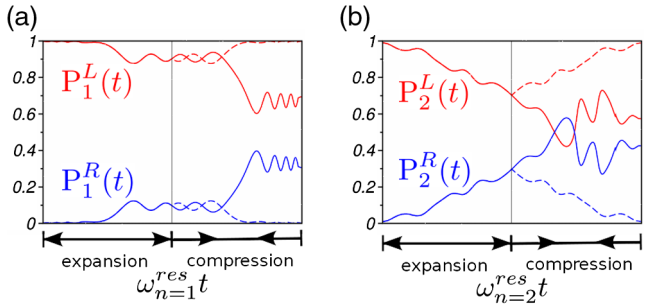

FIG. 2. Particle occupations $P_n^L = \int_{-\infty}^{0} |\Psi(x)|^2 dx$ and $P_n^R = \int_0^{\infty} |\Psi(x)|^2 dx$ for the left-side (red) and right-side (blue) quantum wells during a single expansion-compression stroke. Solid lines represent evolution without time reversal and dashed lines describe the microreversibility effect. The effect is shown for the first ($n = 1$) (a) and second ($n = 2$) (b) LZ anticrossings.

$$\hat{\rho}(0) = \sum_k \frac{e^{-\beta \mathcal{E}_k(\lambda_0)}}{Z(\lambda_0)} |\phi_k(\lambda_0)\rangle\langle\phi_k(\lambda_0)|, \tag{8}$$

where $\beta = 1/k_B T$, $Z(\lambda_0)$ is the partition function and $p_k(\lambda_0) \equiv e^{-\beta \mathcal{E}_k(\lambda_0)}/Z(\lambda_0)$ are the Gibbs ensemble probabilities of the unperturbed system. The system is then isolated from the heat reservoir and undergoes work strokes described by the unitary transformation $\mathcal{U}(t, 0)$. Therefore, $p_k(t) = p_k(\lambda_0)$ and only the quantum states evolve in time to yield $\hat{\rho}(t) = \sum_n p_k(\lambda_0)|\Psi_k(t)\rangle\langle\Psi_k(t)| \equiv \sum_k p_k(\lambda_0)\hat{\rho}_k(t)$. Thus, to study the quantum properties we focus on the matrix $\hat{\rho}_k(t)$ before taking the ensemble average. For the quantum state $|\Psi_k(t)\rangle = \mathcal{U}(t, 0)|\phi_k(\lambda_0)\rangle = \sum_n C_n^k(t)|\phi_n(\lambda_t)\rangle$, in the representation of the adiabatic eigenstates, we have $\rho_{n,m}^k(t) = C_n^k(t)[C_m^k(t)]^*$. The average energy of the quantum system is given by $E_k(t) = \mathrm{Tr}[\rho_k(t)\mathcal{H}(t)] = \sum_n |C_n^k(t)|^2 \mathcal{E}_n(t)$; notice that the work stroke is a nonequilibrium process. If the isolated quantum system undergoes a finite time process, driven by the time-dependent Hamiltonian $\mathcal{H}[\lambda(t)]$, within the time interval $t \in [0, \tau]$, the change of energy is

$$\Delta E_k = \int_0^{\tau} \{\mathrm{Tr}[\dot{\rho}_k(t)\mathcal{H}(t)] + \mathrm{Tr}[\rho_k(t)\dot{\mathcal{H}}(t)]\} dt. \tag{9}$$

However, for a work stroke that is carried out on a thermally isolated system, the energy exchanged with the bath (heat) is zero. In fact, $\mathcal{Q}_k = \int_0^{\tau} \mathrm{Tr}[\dot{\rho}_k(t)\mathcal{H}(t)]dt = 0$, which can be demonstrated by substituting $\dot{\rho}_k(t) = (i/\hbar)[\rho_k(t), \mathcal{H}(t)]$ into the previous equation. Therefore, we have for the work stroke on a thermally isolated quantum system

$$\dot{E}_k = \dot{\mathcal{W}}_k = \mathrm{Tr}[\rho_k(t)\dot{\mathcal{H}}(t)] \tag{10}$$

$$= \dot{\mathcal{W}}_{\mathrm{pop}} + \dot{\mathcal{W}}_{\mathrm{coh}} = \sum_n (P_n^k \dot{\mathcal{E}}_n + \dot{P}_n^k \mathcal{E}_n), \tag{11}$$

where $P_n^k = |C_n^k(t)|^2$. Note that $\mathcal{W}$, in Eq. (11), denotes the work done on the system. Thus by making use of Eq. (3) in Eq. (11), the work exchanged with the quantum system during a finite time process can be written as

$$\mathcal{W}_k = \int_0^{\tau} \left(\sum_n P_n^k \frac{\partial \mathcal{E}_n}{\partial \lambda} + 2 \sum_{n>m} \mathrm{Re}(\rho_{n,m}^k) \times \langle \phi_n | \partial_\lambda \phi_m \rangle (\mathcal{E}_m - \mathcal{E}_n) \right) \dot{\lambda} dt, \tag{12}$$

where $\dot{\mathcal{W}}_{\mathrm{coh}} = \sum_n \dot{P}_n^k \mathcal{E}_n$ is explicitly written, with $\partial_\lambda \equiv \partial/\partial_\lambda$. The first term on the right-hand side of Eq. (12) is herein denoted $\mathcal{W}_{\mathrm{pop}}$ because it depends on the populations $P_n^k(t)$ of the adiabatic states; it could also be associated with incoherent work for systems in equilibrium with a thermal bath. On the other hand, the term $\mathcal{W}_{\mathrm{coh}}$ is nonzero only if there are quantum coherences in the working fluid, as evinced by the off-diagonal elements $\rho_{n,m}^k$. In addition, this term also depends on the rate of the work stroke through the nonadiabatic coupling term $\langle \phi_n | \dot{\phi}_m \rangle$. For instance, if work is performed in the quasistatic (quantum-adiabatic) regime this term vanishes.

The term $\dot{\mathcal{W}}_{\mathrm{coh}}$ is associated in some studies with the notion of work carried out against an inner quantum friction [9–11]. If a working medium is not completely controllable by the external field, thus $[\mathcal{H}(t + \delta t), \mathcal{H}(t)] \neq 0$ and quantum coherences arise [12,29,30] (see Supplemental Material [28]). It has also been pointed out [9] that performance characteristics for such a system can be described as a quantum engine subject to a phenomenological inner friction. We determine the reaction force produced on the movable wall (control parameter) due to the creation of quantum coherences in the working medium and, then, calculate the work performed against this force. The force exchanged between the quantum system and the work repository due to $\dot{\mathcal{W}}_{\mathrm{coh}}$ is obtained from Eq. (12) as

$$\mathcal{F}_{\mathrm{coh}}^k = 2 \sum_{n>m} \mathrm{Re}(\rho_{n,m}^k) \langle \phi_n | \partial_\lambda \phi_m \rangle (\mathcal{E}_m - \mathcal{E}_n). \tag{13}$$

It can be calculated analytically for the present model by using the Hellmann-Feynman theorem on $\partial_\lambda \langle \phi_n | \mathcal{H} | \phi_m \rangle$,

$$\langle \phi_n | \partial_\lambda \mathcal{H} | \phi_m \rangle = \partial_\lambda \mathcal{E}_m(\lambda) \delta_{n,m} + (\mathcal{E}_m - \mathcal{E}_n) \mathbf{d}_{n,m}, \tag{14}$$

where $\mathbf{d}_{n,m} \equiv \langle \phi_n | \partial_\lambda \phi_m \rangle = -\langle \phi_m | \partial_\lambda \phi_n \rangle$. The first term on the right side of Eq. (14) describes the adiabatic force exchanged with the work repository for work strokes performed in the quantum-adiabatic regime, $\omega \ll \omega_{\mathrm{res}}$, while the second term is associated with the population transfer between adiabatic eigenstates. The former constitute diagonal matrix elements whereas the later give rise to off-diagonal matrix elements; notice that $d_{n,n} = 0$, for $\partial_\lambda \langle \phi_n(\lambda) | \phi_n(\lambda) \rangle = 0$. We shall focus on the nonadiabatic off-diagonal terms that yield $\mathbf{d}_{n,m} = \langle \phi_n | \partial_\lambda \phi_m \rangle = \langle \phi_n | \partial_\lambda \mathcal{H} | \phi_m \rangle / (\mathcal{E}_m - \mathcal{E}_n)$, for $n \neq m$. Substitution of $\mathbf{d}_{n,m}$

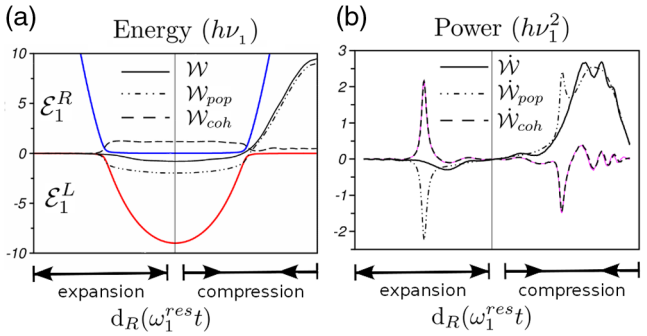

FIG. 3. (a) Energy variation of the quantum system during a single expansion-compression work stroke: $\Delta E = \mathcal{W} = \mathcal{W}_{\rm pop} + \mathcal{W}_{\rm coh}$. Also shown for guidance, the time evolution of the adiabatic energies $\mathcal{E}_1^R$ (blue) and $\mathcal{E}_1^L$ (red). Process carried out in resonance with the first ($n = 1$) LZ anticrossing. (b) Power exchanged with the work repository. The blue line is $\mathcal{F}_{\rm coh} d\lambda/dt$ (magenta line), with $\mathcal{F}_{\rm coh}$ given by Eq. (15).

into Eq. (13) yields $\mathcal{F}^k_{\rm coh} = 2\sum_{n>m} {\rm Re}(\rho^k_{n,m})\langle\phi_n|\partial_\lambda\mathcal{H}|\phi_m\rangle$ and then, by making use of Eqs. (1) and (2), we have $\langle\phi_n|\partial_\lambda\mathcal{H}|\phi_m\rangle = -V\phi_n(\lambda)\phi_m(\lambda)$, where, in the present model, λ stands for the position of the movable wall (or width of the right-side quantum well). Also notice that $\phi_n(x;\lambda_t)$ and $\phi_m(x;\lambda_t)$ are real eigenfunctions of the Hamiltonian $\mathcal{H}(\hat{x};\lambda(t))$. Therefore,

$$\mathcal{F}^k_{\rm coh} = -2V\sum_{n>m} {\rm Re}(\rho^k_{n,m})\phi_n(\lambda_t)\phi_m(\lambda_t). \qquad (15)$$

The average nonadiabatic reaction force acting on the wall of the quantum well is calculated with the Gibbs ensemble weights as $\mathcal{F}_{\rm coh} = \sum_k p_k \mathcal{F}^k_{\rm coh}$. Note that the force [Eq. (15)] is due to quantum coherences built in the working medium by the work stroke, $\dot{\mathcal{W}}_{\rm coh} = \mathcal{F}_{\rm coh}\dot{\lambda}$.

Two-level systems.—Let us analyze the work performed at the lowest Landau-Zener transition. We consider an expansion-compression work stroke by which the width of the movable quantum well, $d_R \equiv \lambda$, changes according to $d_R(t) = d_L[1 - \cos(\omega t)/2]$. Figures 3(a) and 3(b) describe a work stroke performed at the frequency $\omega^{\rm res}_{n=1}$ analogous experiments are performed with SC flux qubits [25,26] by applying a radio frequency (rf) field to drive the qubit back and forth through avoided crossings, and likewise with charge qubits driven by rf gate charge sweeps [27]. Starting from the ground state $|\phi_1^L\rangle$, the LZ passage puts the system in a quantum coherent state. However, the subsequent compression does not restore the system to its original state. The average energy E does not follow the adiabatic path either, which is described in Fig. 3(a) by the evolution of the adiabatic energies $\mathcal{E}^{L,R}_{n=1}$ (red and blue curves)—the behavior for quasistatic (adiabatic) and sudden (nonadiabatic) processes are presented in the Supplemental Material [28]. For the resonant regime, there is considerable power consumed to produce quantum coherences, which is associated with the phenomenological inner friction. As a consequence, $\mathcal{W}_{\rm coh} > 0$ and $|\Delta E| < |\mathcal{W}_{\rm pop}|$; thus, the efficiency for work output is decreased during the expansion stroke, and partially restored during the compression; herein work output means the total work performed during each cycle. Figure 3(b) shows the behavior of the power exchanged during the stroke, $\dot{\mathcal{W}} = \dot{\mathcal{W}}_{\rm pop} + \dot{\mathcal{W}}_{\rm coh}$. Notice that $\dot{\mathcal{W}}_{\rm coh}$ changes sign for expansion and compression. For the sake of comparison we plotted together $\dot{\mathcal{W}}_{\rm coh} = \dot{E} - \dot{\mathcal{W}}_{\rm pop}$ (black dashed line) and $\mathcal{F}_{\rm coh}\dot{\lambda}$ (magenta line), with $\mathcal{F}_{\rm coh}$ given by Eq. (15).

Work fluctuations.—An important issue for mesoscopic engines, both quantum and classical, is the work fluctuation distribution after a sequence of driving cycles [31]. Assume that the system is described at $t = 0$ by the thermalized density matrix given by Eq. (8). Then, during the work stroke it is isolated from the thermal bath (or put into a weak coupling environment), so that the unitary transformation $\mathcal{U}$ holds. Therefore, we can use [15,16]

$$P(\mathcal{W}) = \sum_{n,m} \delta(\mathcal{W} - [\mathcal{E}_m - \mathcal{E}_n])|C^n_m(\tau)|^2 \frac{e^{-\beta\mathcal{E}_n(\lambda_0)}}{Z(\lambda_0)} \qquad (16)$$

to calculate the work fluctuation distribution. For the cyclic expansion-compression stroke $\mathcal{H}(\lambda_\tau) = \mathcal{H}(\lambda_0)$; therefore, the adiabatic basis set is the same at λ_0 and at λ_τ. Thus Eq. (16) simplifies to

$$P(\mathcal{W}) = \frac{1}{Z(\lambda_0)} \sum_{n,m} \delta(\mathcal{W} - [\mathcal{E}_m - \mathcal{E}_n])|C^n_m(\tau)|^2 e^{-\beta\mathcal{E}_n(\lambda_0)}. \qquad (17)$$

For a series of periodic expansion-compression cycles, we verify that the work distribution satisfies the Jarzynski-Bochkov-Kuzovlev equality $\langle e^{-\beta\mathcal{W}}\rangle = \int P(\mathcal{W})\exp(-\beta\mathcal{W})d\mathcal{W} = 1$. Notice that our definition of work, $d\mathcal{H}(\lambda_t)/dt = \mathcal{F}d\lambda/dt$, which is more appropriate for describing an engine, corresponds to the framework used by Bochkov and Kuzovlev [18] in their original paper. The Supplemental Material [28] presents $P(\mathcal{W})$, obtained with Eq. (17) for various initial temperatures after 20 expansion-compression cycles.

Equivalence with flux qubit.—To conclude we consider the functional equivalence of the quantum piston engine and a rf-SQUID flux qubit. The concept is herein presented for a symmetric double quantum well system [Fig. 4(a)], where the focus is on the doublet formed by the symmetric (S) and antisymmetric (AS) states that constitute the lowest 2-level system. The model system is equivalent to a flux qubit biased by an external static magnetic flux $\Phi_{\rm ext} = \Phi_0/2$, [19,20] coupled to an electromagnetic (em) resonator [5,32] that drives the qubit with a rf, as shown in Fig. 4(b). Let us consider that one of the walls oscillates with a small amplitude (1% of the QW width) at the resonant frequency $\omega = \omega_{01}$ of the doublet, then work

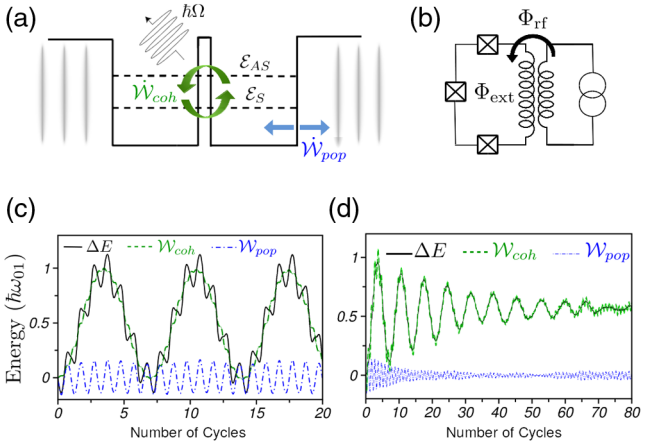

FIG. 4. (a) Symmetric double quantum well (DQW) system and the doublet formed by symmetric (S) and antisymmetric (AS) states (well width is 100 Å, barrier width is 45 Å, potential height is 250 meV, $\hbar\omega_{01} = 1.7253$ meV). (b) Scheme of a rf-SQUID flux qubit. (c) Work exchange $\Delta E = \mathcal{W}_{\rm pop} + \mathcal{W}_{\rm coh}$ without dephasing noise. (d) Work exchange with dephasing noise.

is done on the system in two ways [Fig. 4(c)]: a classicalike work component $\mathcal{W}_{\rm pop} = \sum_n \int P_n \dot{\mathcal{E}}_n dt$ that follows the driving with ω_{01} (blue dot-dashed line), and work $\mathcal{W}_{\rm coh} = \int \mathcal{F}_{\rm coh}\dot{\lambda}dt$ that produces coherent energy that oscillates with the Rabi frequency $\Omega = \gamma/\hbar$ (green dashed line), where γ is associated with the strength of the LZ transition. The coherent energy ($\mathcal{W}_{\rm coh}$) could, in principle, be transferred to a second em resonator coupled to the SQUID and measured with a dc-SQUID magnetometer, whereby the corresponding $\mathcal{F}_{\rm coh}$ could be obtained. We then analyze how the quantum piston is affected by extrinsic dephasing (relaxation time T_2^*), such as noise from the leads that are coupled to read-out devices or used to apply flux or charge biases. Thus, we apply a classical Gaussian noise to the driving parameter, $\dot{\lambda}(t) = (\lambda_0\omega_{01}/100)\cos[(\omega_{01} + \varphi(t))t]$, with noise distribution $P(\varphi) \propto \exp(-\varphi^2/2\omega_{01}^2)$, then, an ensemble average over 78 trajectories is carried out. We observe that this dephasing in the driving decreases the amplitude of the quantum coherent signal, which decays exponentially with $\Gamma_2^* \approx 0.03\Omega$ [Fig. 4(d)].

The authors are grateful for financial support from CNPq and FAPESC.

[1] K. E. Dorfman, D. V. Voronine, S. Mukamel, and M. O. Scully, Proc. Natl. Acad. Sci. U.S.A. **110**, 2746 (2013).
[2] P. J. M. Johnson, A. Halpin, T. Morizumi, O. P. E. Valentyn I. Prokhorenko, and R. J. D. Miller, Nat. Chem. **7**, 980 (2015).
[3] A. Chenu and G. Scholes, Annu. Rev. Phys. Chem. **66**, 69 (2015).
[4] P. Kukura, D. W. McCamant, S. Yoon, D. B. Wandschneider, and R. A. Mathies, Science **310**, 1006 (2005).
[5] M. H. devoret and J. M. Martinis, Quantum Inf. Process. **3**, 163 (2004).
[6] R. J. Schoelkopf and S. M. Girvin, Nature (London) **451**, 664 (2008).
[7] F. Yans, S. Gustavsson, A. Kamal, J. Birenbaum, A. P. Sears, D. Hover, T. J. Gudmundsen, D. Rosenberg, G. Samach, S. Weber, J. L. Yoder, T. P. Orlando, J. Clarke, A. J. Kerman, and W. D. Oliver, Nat. Commun. **7**, 12964 (2016).
[8] S. O. Valenzuela, W. D. Oliver, D. M. Berns, K. K. Berggren, L. S. Levitov, and T. P. Orlando, Science **314**, 1589 (2006).
[9] R. Kosloff and T. Feldmann, Phys. Rev. E **65**, 055102 (2002).
[10] Y. Rezek and R. Kosloff, New J. Phys. **8**, 83 (2006).
[11] F. Plastina, A. Alecce, T. J. G. Apollaro, G. Falcone, G. Francica, F. Galve, N. Lo Gullo, and R. Zambrini, Phys. Rev. Lett. **113**, 260601 (2014).
[12] R. Uzdin, A. Levy, and R. Kosloff, Phys. Rev. X **5**, 031044 (2015).
[13] T. Feldmann and R. Kosloff, Phys. Rev. E **61**, 4774 (2000).
[14] C. Jarzynski, Phys. Rev. Lett. **78**, 2690 (1997).
[15] P. Talkner, P. Hänggi, and M. Morillo, Phys. Rev. E **77**, 051131 (2008).
[16] M. Campisi, P. Hänggi, and P. Talkner, Rev. Mod. Phys. **83**, 771 (2011).
[17] M. Campisi, P. Talkner, and P. Hänggi, Phil. Trans. R. Soc. A **369**, 291 (2011).
[18] G. Bochkov and Y. Kuzovlev, Physica (Amsterdam) **106A**, 443 (1981).
[19] J. Clarke and F. K. Wilhelm, Nature (London) **453**, 1031 (2008).
[20] C. H. van der Wal, A. C. J. ter Haar, F. K. Wilhelm, R. N. Schouten, C. J. P. M. Harmans, T. P. Orlando, S. Lloyd, and J. E. Mooij, Science **290**, 773 (2000).
[21] A. Torres, R. S. Oliboni, and L. G. C. Rego, J. Phys. Chem. Lett. **6**, 4927 (2015).
[22] R. S. Oliboni, G. Bortolini, A. Torres, and L. G. C. Rego, J. Phys. Chem. C **120**, 27688 (2016).
[23] N. V. Vitanov, Phys. Rev. A **59**, 988 (1999).
[24] F. Brito, F. Rouxinol, M. D. LaHaye, and A. O. Caldeira, New J. Phys. **17**, 075002 (2015).
[25] W. D. Oliver, Y. Yu, J. C. Lee, K. K. Berggren, L. S. Levitov, and T. P. Orlando, Science **310**, 1653 (2005).
[26] D. M. Berns, W. D. Oliver, S. O. Valenzuela, A. V. Shytov, K. K. Berggren, L. S. Levitov, and T. P. Orlando, Phys. Rev. Lett. **97**, 150502 (2006).
[27] M. Sillanpää, T. Lehtinen, A. Paila, Y. Makhlin, and P. Hakonen, Phys. Rev. Lett. **96**, 187002 (2006).
[28] See Supplemental Material at http://link.aps.org/supplemental/10.1103/PhysRevLett.119.090601 for supporting information.
[29] R. Kosloff and A. Levy, Annu. Rev. Phys. Chem. **65**, 365 (2014).
[30] G. Katz and R. Kosloff, Entropy **18**, 186 (2016).
[31] M. Campisi, J. Phys. A **47**, 245001 (2014).
[32] M. J. Everitt, P. Stiffell, T. D. Clark, A. Vourdas, J. F. Ralph, H. Prance, and R. J. Prance, Phys. Rev. B **63**, 144530 (2001).